Finite Element Analysis of Creep Crack Initiation in Functionally Graded Materials with Crack Parallel to the Gradient

Huan Sheng Lai[1,*], Chunmei Bai[2] and Kang Lin Liu[3]

[1]*Sino-French Institute of Nuclear Engineering and Technology, Sun Yat-sen University, Zhuhai 519082, China*

[2]*School of Civil Engineering, Sun Yat-sen University, Zhuhai 519082, China*

[3]*School of Chemical Engineering, Fuzhou University, Fujian 350116, China*

Abstract: With the advances in material synthesis technologies, functionally graded materials (FGMs) are developed to use in high temperature structurals due to the excellent high temperature mechanical properties. To facilitate wide use of FGMs in high temperature structures, finite element method (FEM) was used in this paper to investigate effects of creep resistant properties gradients on creep crack initiation (CCI) in FGMs, with crack parallel to the gradient. Results indicated that when creep resistant properties increased in the crack growth direction, CCI was retarded by creep properties gradients. However, CCI was accelerated by creep properties gradients when creep resistant properties decreased in the crack growth direction. CCI position occurred in the two symmetric slanted planes of the initial crack, regardless of the gradient variation of creep resistant properties.

Keywords: FGM, creep damage, creep crack initiation, functionally graded material.

1. INTRODUCTION

Functionally graded materials (FGMs) have gradient material properties in one or more directions [1, 2]. Bamboo which is a kind of nature FGMs has been used in construction engineering for thousands of years, and its creep behavior is researched by Gottron [3]. Recent advances in material synthesis technologies have spurred development of FGMs. The creep behavior of FGMs has attracted attention of many researchers due to the outstanding characteristics of these structures in high temperature applications, such as FGM-rotating discs which is used in steam and gas turbine rotors, pumps, compressors, and fly-wheels as well as FGM cylinders that are used in aerospace industries and nuclear reactors. Singh [4], Gupta [5], and, Deepak [6] found that a FGM-rotating disc had smaller steady state creep rates than a homogeneous material rotating disc. Mangal [7] and Singh [8] reported that creep rates in FGM cylinders were lower in comparison with homogeneous cylinders. Methods to calculate stresses and creep strain rates in FGM cylinders and spheres have been reported by numerous authors [9-15]. For creep crack in FGMs, Chen [16] used finite element method (FEM) to research creep crack in functionally graded coatings and found that the crack tip stress field could be characterized by C^* under extensive steady state creep stage. Interlayer of multilayered systems with an interfacial crack was assumed to have functionally graded creep resistant properties in the work reported by Xuan [17]. Lai [18, 19] proposed estimation methods of C_t, $C(t)$ and creep crack tip stress field of FGMs. Xu [20] experimentally investigated creep crack growth (CCG) behavior in Al/Al-4wt%Cu FGM, where the crack was parallel to material properties gradients, and discovered that CCG was retarded. Even though fracture mechanics of FGMs have been studied extensively, focus has mainly been on elastic-plastic fracture field [21-24]. Effects of creep resistant properties gradients on creep crack initiation (CCI) are still unknown. The time of CCI is an important performance to evaluate the creep life and ensure the safety of FGMs used in high temperature structures. To guide the development of FGMs and facilitate wide use of FGMs in high temperature structures, it is critical to understand the effect of creep resistant properties gradients on CCI in FGMs.

In this paper, effects of creep resistant properties gradients on CCI in FGMs have been studied using FEM. The analysis was carried out using the commercial software Abaqus. Numerical simulation was used here, primarily due to the fact that it is an effective and powerful method to analyze fracture of FGMs [25-27]. Here, crack parallel to the gradient were studied and various kinds of creep resistant properties gradients were used to discuss their effects on CCI in FGMs.

2. FINITE ELEMENT ANALYSIS

2.1. Model for Creep Damage

Creep damage parameter, w, was defined [28] such that $0 \le w \le 1$ and failure occurred when $w = 1$.

*Address correspondence to this author at the Sino-French Institute of Nuclear Engineering and Technology, Sun Yat-sen University, Zhuhai 519082, China; Tel: +86-020-8411-2828; Fax: +86-020-8411-2828;
E-mail: sheng158@hotmail.com

E-ISSN: 2409-9821/19

Relationship between the creep damage rate, $\dot{w}$, and the equivalent creep strain rate, $\dot{\varepsilon}_c$, is expressed as:

$$\dot{w} = \frac{\dot{\varepsilon}_c}{\varepsilon_f^*} \tag{1}$$

where ε_f^* is the multiaxial creep ductility and can be calculate by [29]:

$$\frac{\varepsilon_f^*}{\varepsilon_f} = \sinh\left[\frac{2}{3}\left(\frac{n-0.5}{n+0.5}\right)\right] \Big/ \sinh\left[2\left(\frac{n-0.5}{n+0.5}\right)\frac{\sigma_{\mathrm{m}}}{\sigma_{\mathrm{e}}}\right] \tag{2}$$

where σ_{e} is the equivalent stress, σ_{m} is the mean stress, ε_f is the uniaxial creep ductility, and *n* is the power-law creep exponent. Value of $\varepsilon_f^*/\varepsilon_f$ was not significantly affected by *n*, when *n* was larger than five [30]. Since no work has been reported in literature which studies the variation of ε_f in FGMs, it is not easy to simulate the creep crack growth in FGMs. Therefore, in this paper, all cases were assumed to have the same material properties at the crack tip and ε_f was fixed at 0.49 at the crack tip.

At any instant, *w* is the integral of $\dot{w}$ up to that time, *t*:

$$w = \int_0^t \dot{w} dt \tag{3}$$

Since crack tip region has the highest equivalent creep strain rate, failure occurs in the region of the crack tip when $w = 1$.

2.2. Specimen Geometry and Material Properties

Standard single edge bend [SE(B)] specimens for FGMs were studied as shown in Figure **1**, where the creep crack was parallel to the material properties gradients, denoted as 'crack parallel to the gradient'. Detailed dimensions of the specimens are shown in Figure **1**.

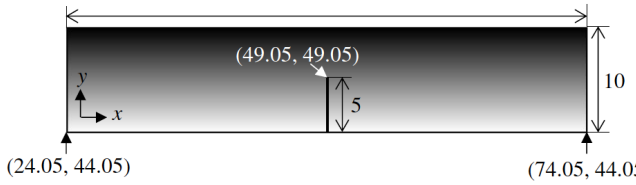

Figure 1: Standard SE(B) specimen with crack parallel to the gradient (specimen thickness was 5 mm); unit: mm.

Based on the observations of the creep damage model [Eqs. (1-3)], it was found that creep damage was mainly dependent on the creep strain rate and the value of stress triaxiality of $\sigma_{\mathrm{m}}/\sigma_e$. Thus, effects of elastic properties gradients on the creep damage were too small to be ignored. Therefore, elastic properties of Poisson's ratio, *v*, and Young's modulus, *E*, were fixed at 0.3 and 179.4 GPa, respectively. Creep properties were assumed only through the *y*-axis graded direction and by obeying the power-law gradient. The creep constitutive of FGMs was assumed elastic plus power law. Therefore, for crack parallel to the gradient, the total creep strain rate could be given as:

$$\dot{\varepsilon} = \dot{\sigma}_e / E + A(y)\sigma_e^{n(y)} \tag{4}$$

where $A(y) = A_0 y^{A_1}$ and $n(y) = n_0 y^{n_1}$.

In the above equations, $\dot{\varepsilon}$ is the total creep strain rate. $\dot{\sigma}_e$ is the equivalent stress rate. *A*(*y*) and *n*(*y*) are the *y* coordinate-dependent power-law creep coefficient and exponent, respectively. A_0, A_1, n_0, and n_1 are constants. As shown in Figure **1**, all SE(B) specimens had the same coordinate values of *x*, ranging from 24.05 mm to 74.05 mm, and *y*, ranging from 44.05 mm to 54.05 mm; crack tip was located at (49.05 mm, 49.05 mm).

Table **1** shows creep properties of all cases used in this research [18]. They all had the same material properties at the crack tip. In particular, case 1 was a homogeneous specimen made of a homogeneous material. The results of FGM cases were discussed in comparison with case 1. For cases with crack parallel to the gradient, as shown in Table **1**, creep properties decreased in the crack growth direction when A_1 or n_1 was negative, and vice versa. For example, *A* with negative A_1 decreased in the crack growth direction and *n* with positive n_1 increased in the crack growth direction for case 8. Therefore, creep resistant properties in cases 2 – 4 increased in the crack growth direction, while creep resistant properties in cases 5 – 7 decreased in the crack growth direction. The reason was that the larger creep properties meant the smaller creep resistant properties. Gradient variations of *A* and *n* were completely opposite for cases 8 and 9, as shown in Table **1**. Therefore, they had mixture of creep resistant properties gradients.

2.3. Finite Element Model

Commercial finite element program Abaqus was used to simulate a three-point bend test in order to investigate the effects of creep resistant properties gradients on CCI in FGMs. All cases used the same finite element model for SE(B) specimens, as shown in

Table 1: Creep Properties of all Cases [18]

Case	$A(y)$ MPa^{-n}/h		$n(y)$	
	A_0	A_1	n_0	n_1
1	1.36E-24	0	10.94	0
2	1.10E-37	-10	10.94	0
3	1.36E-24	0	3.28	-0.4
4	1.10E-37	-10	3.28	-0.4
5	1.69E-11	10	10.94	0
6	1.36E-24	0	36.55	0.4
7	1.69E-11	10	36.55	0.4
8	1.10E-37	-10	36.55	0.4
9	1.69E-11	10	3.28	-0.4

Figure **2**. Since the grain size was about 50 μm for high temperature materials [31], the region ahead of the crack tip had finer square meshes with size of 20 μm, as shown in Figure **2b**. Finer meshes at the crack tip could avoid mesh dependency effects in the simulation [31] and was needed in order to simulate crack growth in FGMs due to large strain gradients [32, 33]. The model includes 15588 elements. Element type was CPE4, which is a four-node and plane strain element. The crack tip was initially sharp. As in actual experiments, for the simulation, the specimen was supported by two rigid pins and a load was applied to the specimen using a rigid loading pin. Surface friction coefficient between the pin and specimen was fixed at 0.3. All applied loads were fixed at -200 N. Span length between the two supporting pins was 45 mm.

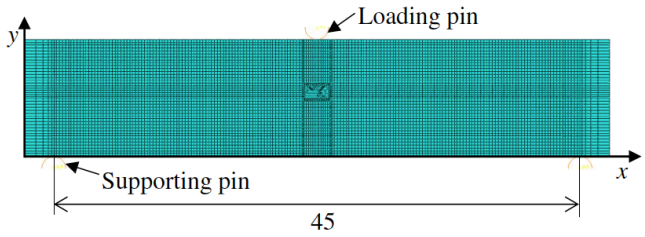

(a) Meshes of the whole model

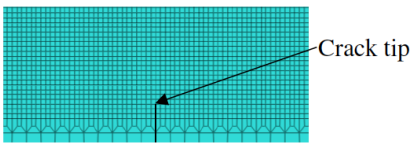

(b) Meshes around the crack tip

Figure 2: Finite element model of the three-point bent test for SE(B) specimens.

Two user defined field subroutines (USDFLD) were compiled and implemented into Abaqus. One was to achieve creep resistant properties gradients [18]. The other was to simulate CCI in FGMs based on the model for creep damage from part 2.1. In the latter subroutine, the Young's modulus of failure nodes with $w = 1$ was set to 0.1 MPa in order to reduce their load-carrying capacity. This method has been widely used by others [34-36]. The computations were performed with explicit algorithms.

3. RESULTS AND DISCUSSION

3.1. Crack in Homogeneous Material

Development of w for case 1 of a homogeneous specimen is shown in Figure **3**. w was very small and its maximum value was less than 1 at t = 108.1 h, as shown in Figure **3a**. When t = 298.1 h, two failure nodes with w = 1 were first observed in the two symmetric slanted planes of the initial crack, as shown in Figure **3b**. This was observed because concentration of equivalent creep strain CEEQ did not occur ahead of the crack tip for an initial sharp crack [37], as shown in Figure **3** for the development of CEEQ. This phenomenon was first realized by Rice [38] and also observed by Ozmat as shown in Figure **4** [39]. With the increase in creep time, the initial sharp crack tip became blunt and the failure nodes began to appear in the symmetry plane of the crack. Therefore, the damage first appeared in the two symmetric slanted planes of the initial crack, and then appeared in the symmetry plane, as shown in Figure **3c**. The time that failure nodes first appeared was referred to as CCI time, t_i, and the position of the failure nodes was CCI position. Note that CCI position of a creep crack was affected by crack geometries [37, 40].

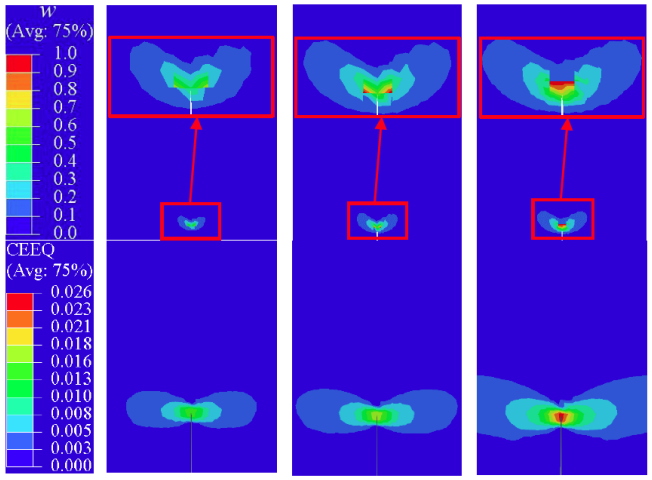

(a) t = 108.1 h (b) t = 298.1 h (c) t = 426.6 h

Figure 3: Development of creep damage and CEEQ of case 1 of a homogeneous specimen.

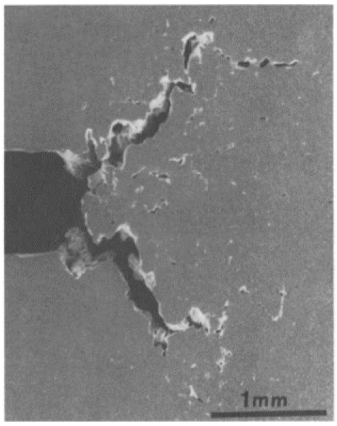

Figure 4: Experimental observation of initial creep crack growth for specimen with initial sharp crack [38].

3.2. Crack in FGM

Development of *w* for case 2, with increased creep resistant properties in the crack growth direction, is shown in Figure **5**. As shown in Figure **5b**, two failure nodes were first observed in the two symmetric slanted planes of the initial crack at *t* = 435.7 h. After that, failure nodes were found at the crack tip, as shown in Figure **5c**. The damage contour and CEEQ contour were symmetric to the medium plane of the initial crack and were similar to case 1 (Figure **3**). Development of *w* and CEEQ of other cases, with crack parallel to the gradient, were similar to case 2. Therefore, to avoid repetition, they are not shown in this paper.

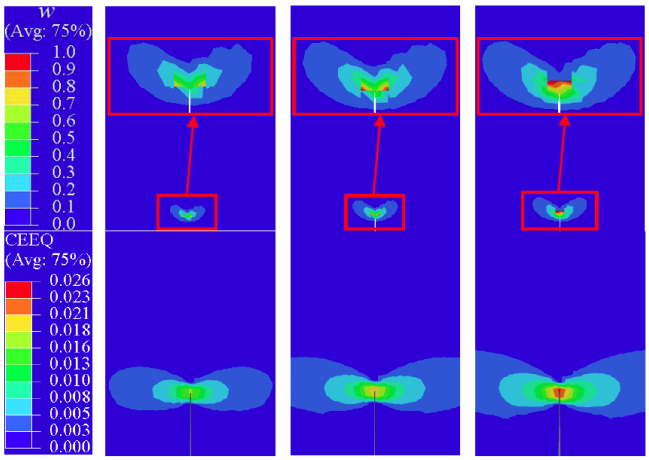

Figure 5: Development of creep damage and CEEQ of case 2 with crack parallel to the gradient and increased creep resistant properties in the crack growth direction.

Table **2** and Figure **6** show t_i for all the cases. t_i was normalized by t_0 in Figure **6**, where t_0 was t_i of case 1. As shown in Figure **6**, t_i of cases 2 – 4 was larger than t_0. Creep properties in cases 2 – 4 decreased in the crack growth direction. It is known that creep resistance increases with smaller creep properties and vice versa. This implies that their creep resistance increased in the crack growth direction and increased with an increase in the magnitude of creep properties gradients. Since all cases had the same material properties at the crack tip, creep resistance of cases 2 – 4 was stronger than case 1. Cases 2 – 4 hence needed longer time for CCI. Creep properties gradients of case 4 were the sum of cases 2 and 3. As a result, case 4 had a stronger creep resistance and had larger t_i than cases 2 and 3. It could be deduced that case 3 had a higher magnitude of creep properties gradients and stronger creep resistance than case 2, because case 3 had larger t_i than case 2. Therefore, t_i was increased by creep properties gradients and increased with an increase in the magnitude of creep properties gradients for cases with increased creep resistant properties in the crack growth direction.

Table 2: Creep Crack Initiation Time of all Cases

Case	t_i h	Case	t_i h
1	298.1	6	150.2
2	435.7	7	102.7
3	566.4	8	225.1
4	830.3	9	376.9
5	196.9		

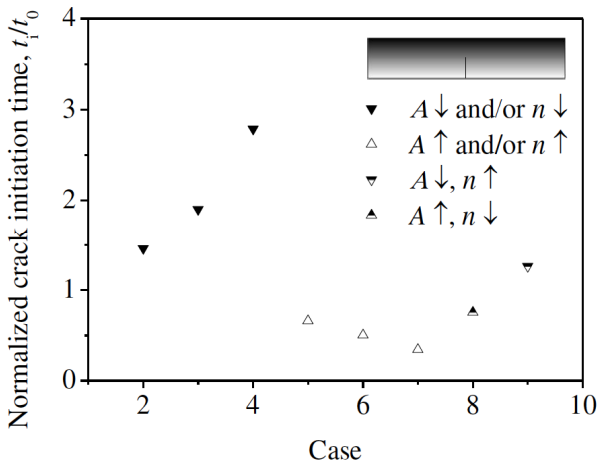

Figure 6: Normalized creep crack initiation time of cases with crack parallel to the gradient; ↑ – increased creep properties in the crack growth direction; ↓ – decreased creep properties in the crack growth direction.

For cases with decreased creep resistant properties in the crack growth direction, t_i of cases 5 – 7 was

smaller than t_0, as shown in Table **2** and Figure **6**. The reason was that creep resistant properties in cases 5 – 7 decreased in the crack growth direction. This means that their creep resistance was weaker than case 1 and decreased with an increase in the magnitude of creep properties gradients. Hence, they needed only shorter time for CCI in comparison with case 1. Case 6 had a higher magnitude of creep properties gradients and weaker creep resistance than case 5, because case 6 had a smaller t_i than case 5. Since creep properties gradients of case 7 were the sum of cases 5 and 6, creep resistance of case 7 was weaker than cases 5 and 6. Case 7 hence had smaller t_i than cases 5 and 6. Therefore, high the magnitude of creep properties gradients resulted in smaller t_i for cases with decreased creep resistant properties in the crack growth direction. This phenomenon was contrary to the results of cases 2 – 4 with increased creep resistant properties in the crack growth direction.

Cases 8 and 9 had mixture of creep properties gradients in the crack growth direction. t_i of case 8 was smaller than t_0, while t_i of case 9 was larger than t_0, as shown in Table **2** and Figure **6**. These results mean that the gradient of *n* had a higher magnitude than *A* for cases 8 and 9. Only in this way, creep resistance could decrease in the crack growth direction and t_i could be smaller than t_0 for case 8, and the creep resistance could increase in the crack growth direction and t_i could be larger than t_0 for case 9. In other words, the interaction effect of the gradients of *A* and *n* lead to decreased creep resistance in the crack growth direction for case 8. Whereas, for case 9, creep resistance increased in the crack growth direction.

Therefore, it could be concluded that CCI was retarded by creep properties gradients for cases with increased creep resistant properties in the crack growth direction, but it was accelerated by creep properties gradients for cases with decreased creep resistant properties in the crack growth direction. For cases with mixture of creep properties gradients, CCI was dependent on creep properties which had a higher magnitude of gradient.

Since applied load and material properties were symmetric to the median plane of the initial crack, damage contour was symmetric to the median plane of the initial crack and creep crack should propagate along the median plane of the initial crack, for cases with crack parallel to the gradient. The creep crack propagation path for the three-point bend test of Al/Al-4Wt%Cu FGM is shown in Figure **7** [20], where the crack is parallel to the material properties gradients. As shown in Figure **7**, creep crack propagated along the median plane of the initial crack, even though the path was not a straight line. Note that the creep crack propagation path in the FGM was the marked part, the upper part was the path that the creep crack propagated from the pure Al (aluminum) layer to the FGM layer. Therefore, simulated CCI for cases with crack parallel to the gradient agreed with the experimental result.

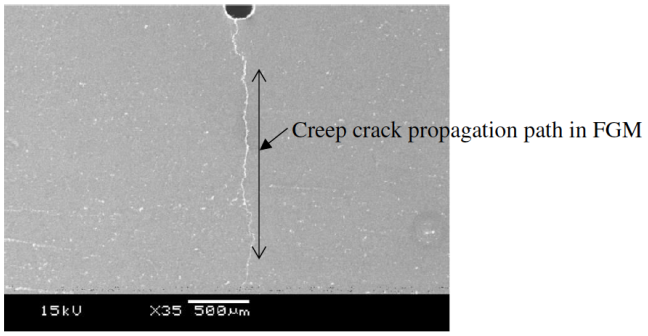

Figure 7: Creep crack propagation path of Al/Al-4Wt%Cu FGM with crack parallel to the gradient [19].

4. CONCLUSIONS

FEM was used to investigate the effects of creep resistant properties gradients on CCI in FGMs, with crack parallel to the gradient. The main conclusions that were made in this study are listed below.

1. When creep resistant properties increased in the crack growth direction, CCI was retarded by creep properties gradients. However, CCI was accelerated by creep properties gradients when the creep resistant properties decreased in the crack growth direction.

2. When the creep properties had mixture of gradients, CCI was dependent on the creep property which had a higher magnitude of gradient.

3. CCI position occurred in the two symmetric slanted planes of the initial crack regardless of the gradient variation of creep properties.

4. This work could guide the development of FGMs and facilitate wide use of FGMs in high temperature structures.

ACKNOWLEDGMENTS

This work was supported by the National Natural Science Foundation of China (51705078) and Qishan

Scholars Program of Fuzhou University in 2016 (XRC-1689).

NOMENCLATURE

A = Power-law creep coefficient

$A(y)$ = y coordinate-dependent power-law creep coefficient of FGMs

A_0, A_1 = Constants

CCG = Creep crack growth

CCI = Creep crack initiation

E = Young's modulus

FGM = Functionally graded material

FEM = Finite element method

n = Power-law creep exponent

$n(y)$ = y coordinate-dependent power-law creep exponent of FGMs

n_0, n_1 = Constants

SE(B) = Single edge bend

t = Creep time

t_i = Creep crack initiation time

t_0 = t_i of case 1 of a homogeneous specimen made of a homogeneous material

v = Poisson's ratio

w = Creep damage

$\dot{w}$ = Creep damage rate

x, y = Global coordinate system of the single edge bend specimens

$\dot{\varepsilon}$ = Total creep strain rate

$\dot{\varepsilon}_c$ = Equivalent creep strain rate

ε_f^* = Multiaxial creep ductility

ε_f = Uniaxial creep ductility

σ_e, $\dot{\sigma}_e$ = Equivalent stress and stress rate, respectively

σ_m = Mean stress

REFERENCES

[1] D.K. Jha, T. Kant, R.K. Sing, A critical review of recent research on functionally graded plates, Compos. Struct. 96 (2013) 833-849. https://doi.org/10.1016/j.compstruct.2012.09.001

[2] J. Li, B.L. Zheng, Q. Yang, X.J. Hu, Analysis on time-dependent behavior of laminated functionally graded beams with viscoelastic interlayer, Compos. Struct. 107 (2014) 30-35. https://doi.org/10.1016/j.compstruct.2013.07.047

[3] Gottron J, Harries KA, Xu Q. Creep behavior of bamboo, Constr. Build Mater. 66 (2014): 79-88. https://doi.org/10.1016/j.conbuildmat.2014.05.024

[4] S.B. Singh, S. Ray, Creep analysis in an isotropic FGM rotating disc of Al-Sic composite, J. Mater. Process. Tech. 143-144 (2003) 616-622. https://doi.org/10.1016/S0924-0136(03)00445-X

[5] V.K. Gupta, S.B. Singh, H.N. Chandrawat, S. Ray, Creep behavior of a rotating functionally graded composite disc operating under thermal gradient, Metall. Mater. Trans. A 35(4) (2004) 1381-1391. https://doi.org/10.1007/s11661-004-0313-3

[6] D. Deepak, V.K. Gupta, A.K. Dham, Creep modeling in functionally graded rotating disc of variable thickness, J. Mech. Sci. Technol. 24(11) (2010) 2221-2232. https://doi.org/10.1007/s12206-010-0817-2

[7] S.K. Mangal, N. Kapoor, T. Singh, Steady-state creep analysis of functionally graded rotating cylinder, Strain 49 (2013) 457-466. https://doi.org/10.1111/str.12052

[8] T. Singh, V.K. Gupta, Modeling steady state creep in functionally graded thick cylinder subjected internal pressure, J. Compos. Mater. 44(11) (2010) 1317-1333. https://doi.org/10.1177/0021998309353214

[9] Y.Y. Yang, Time-dependent stress analysis in functionally graded materials, Int. J. Solids Struct. 37 (2007) 7593-7608. https://doi.org/10.1016/S0020-7683(99)00310-8

[10] L.H. You, H. Ou, Z.Y. Zheng, Creep deformations and stresses in thick-walled cylindrical vessels of functionally graded materials subjected to internal pressure, Compos. Struct. 78 (2007) 285-291. https://doi.org/10.1016/j.compstruct.2005.10.002

[11] S.M.A. Aleayoub, A. Loghman, Creep stress redistribution analysis of thick-walled FGM spheres, J. Solid. Mech. 2(2) (2010) 115-128.

[12] J.J. Chen, S.T. Tu, F.Z. Xuan, Z.D. Wang, Creep analysis for a functionally graded cylinder subjected to internal and external pressure, J. Strain. Anal. Eng. 42 (2007) 69-77. https://doi.org/10.1243/03093247JSA237

[13] A. Loghman, S.A.M. Aleayoub, S.M. Hasani, Time-dependent magnetothermoelastic creep Modeling of FGM spheres using method of successive elastic solution, Appl. Math. Model. 36 (2012) 836-845. https://doi.org/10.1016/j.apm.2011.07.038

[14] M.D. Kashkoli, M.Z. Nejad, Time-dependent thermos-elastic creep analysis of thick-walled spherical pressure vessels made of functionally graded materials, J. Theor. App. Mech-pol. 53(4) (2015) 1053-1065. https://doi.org/10.15632/jtam-pl.53.4.1053

[15] H.L. Dai, H.J. Jiang, L. Yang, Time-dependent behaviors of a FGPM hollow sphere under the coupling of multi-fields, Solid State Sci. 14 (2012) 587-597. https://doi.org/10.1016/j.solidstatesciences.2012.02.011

[16] J.J. Chen, S.T. Tu, Creep fracture parameters of functionally graded coating, J. Chin. Inst. Eng. 27(6) (2004) 805-812. https://doi.org/10.1080/02533839.2004.9670931

[17] F.Z. Xuan, Z.F. Wang, S.T. Tu, Creep finite element simulation of multilayered system with interfacial cracks, Mater. Design. 30 (2009) 563-569. https://doi.org/10.1016/j.matdes.2008.05.067

[18] H.S. Lai, Estimation of Ct of functionally graded materials under small scale creep stage, Compos. Struct. 138 (2016) 352-360. https://doi.org/10.1016/j.compstruct.2015.11.070

[19] H.S. Lai, K.B. Yoon, Estimation of *C*(*t*) and the creep crack tip stress field of functionally graded materials and verification via finite element analysis, Compos. Struct. 153 (2016) 728-737. https://doi.org/10.1016/j.compstruct.2016.07.004

[20] S. Yu, W. Dong, F.M. Xu, M.B. Fu, Y. Tan, Effects of heat treatment on the creep crack growth behavior in Al/Al-4wt%Cu functionally graded material, Adv. Mater. Res. 711 (2013) 81-86. https://doi.org/10.4028/www.scientific.net/AMR.711.81

[21] P. Gu, M. Dao, R.J. Asaro, A simplified method for calculating the crack-tip field of functionally graded materials using the domain integral, J. Appl. Mech-T. ASME 68 (1999) 101-108. https://doi.org/10.1115/1.2789135

[22] Z.H. Jin, N. Noda, Crack-tip singular fields in nonhomogeneous materials, J. Appl. Mech-T. ASME 61 (1994) 738-740. https://doi.org/10.1115/1.2901529

[23] Z.H. Jin, R.C. Batra, Some basic fracture mechanics concepts in functionally graded materials, J. Mech. Phys. Solids 44(8) (1996) 1221-1235. https://doi.org/10.1016/0022-5096(96)00041-5

[24] P. Shanmugavel, G.B. Bhaskar, M. Chandrasekaran, An overview of fracture analysis in functionally graded materials, Eur. J. Sci. Res. 68(3) (2012) 412-439.

[25] C.E. Rousseau, H.V. Tippur, Influence of elastic variations on crack initiation in functionally graded glass-filled epoxy, Eng. Fract. Mech. 69 (2002) 1679-1693. https://doi.org/10.1016/S0013-7944(02)00056-5

[26] C. Comi, S. Mariani, Extended finite element simulation of quasi-brittle fracture in functionally graded materials, Comput. Method. Appl. M. 196 (2007) 4013-4026. https://doi.org/10.1016/j.cma.2007.02.014

[27] M. Fulland, M. Steigemann, H.A. Richard, M. Specovius-Neugebauer, Development of stress intensities for crack in FGMs with orientation perpendicular and parallel to the gradation, Eng. Fract. Mech. 95 (2012) 37-44. https://doi.org/10.1016/j.engfracmech.2011.12.005

[28] M. Yatomi, K.M. Nikbin, N.P. O'Dowd, Creep crack growth prediction using a damage based approach, Int. J. Pres. Ves. Pip. 80 (2003) 573-583. https://doi.org/10.1016/S0308-0161(03)00110-8

[29] A.C.F. Cocks, M.F. Ashby, Intergranular fracture during power-law creep under multiaxial stress, Metal. Sci. 14 (1980) 395-402. https://doi.org/10.1179/030634580790441187

[30] M. Yatomi, Factors affecting the failure of cracked components at elevated temperature [PhD thesis], Imperial College London; (2003).

[31] L. Zhao, H. Jing, Y. Han, J. Xiu, L. Xu, Prediction of creep crack growth behavior in ASME P92 steel welded joint, Comp. Mater. Sci. 61 (2012) 185-193. https://doi.org/10.1016/j.commatsci.2012.04.028

[32] Z.Q. Wang, T. Nakamura, Simulations of crack propagation in elastic-plastic graded materials, Mech. Mater. 36 (2004) 601-622. https://doi.org/10.1016/S0167-6636(03)00079-6

[33] Z.Y. Zhang, G.H. Paulino, Cohesive zone modeling of dynamic failure in homogeneous and functionally graded materials, Int. J. Plasticity. 21 (2005) 1195-1254. https://doi.org/10.1016/j.ijplas.2004.06.009

[34] C.S. Oh, N.H. Kin, Y.J. Kim, C. Davies, K. Nikbin, D. Dean, Creep failure simulations of 316H at 550 °C: Part I – A method and validation, Eng. Fract. Eech. 78 (2011) 2966-2977. https://doi.org/10.1016/j.engfracmech.2011.08.015

[35] N.H. Kim, C.S. Oh, Y.J. Kim, C. Davies, K. Nikbin, D. Dean, Creep failure simulations of 316H at 550 °C: Part II – Effects of specimen geometry and loading mode, Eng. Fract. Mech. 105 (2013) 169-81. https://doi.org/10.1016/j.engfracmech.2013.04.001

[36] M. Tabuchi, H. Hongo, T. Watanabe, A.T. Yokobori Jr, Creep crack growth analysis of welded joints for high Cr heat resisting steel, ASTM STP1480 1480 (2008) 93-101.

[37] K.J. Hsia, A.S. Argon, D.M. Parks, Modeling of creep damage evolution around blunt notches and sharp cracks, Mech. Mater. 11 (1991) 19-42. https://doi.org/10.1016/0167-6636(91)90037-Z

[38] J.R. Rice, M.A. Johnson, The role of large crack tip geometry changes in plane strain fracture, In: Inelastic behavior of Solids, New York; (1970) 641-672.

[39] B. Ozmat, A.S. Argon, D.M. Parks, Growth modes of cracks in creeping type 304 stainless steel, Mech. Mater. 11 (1991) 1-17. https://doi.org/10.1016/0167-6636(91)90036-Y

[40] Y. Luo, W.C. Jiang, Z.Y. Zhang, Y.C. Zhang, W. Woo, S.T. Tu, Notch effect on creep damage for Hastelloy C276-BNi2 brazing joint, Mater. Design. 84 (2015) 212-222. https://doi.org/10.1016/j.matdes.2015.06.111

Received on 09-09-2019 Accepted on 07-10-2019 Published on 18-10-2019

DOI: http://dx.doi.org/10.15377/2409-9821.2019.06.3